

## Incipient Antiferromagnetism and Low-Energy Excitations in the Half-Filled Two-Dimensional Hubbard Model

J. J. Deisz,<sup>1</sup> D. W. Hess,<sup>2</sup> and J. W. Serene<sup>1</sup>

<sup>1</sup>*Department of Physics, Georgetown University, Washington, DC 20057-0995*

<sup>2</sup>*Complex Systems Theory Branch, Naval Research Laboratory, Washington, DC 20375-5345*

(Received 8 March 1995)

We present single-particle and thermodynamic properties of the half-filled single-band Hubbard model in 2D calculated in the self-consistent fluctuation exchange approximation. The low-energy excitations at moderate temperatures and small  $U$  are quasiparticles with a short lifetime. As the temperature is lowered, coupling to evolving spin fluctuations leads to the extinction of these quasiparticles, signaled by a weak pseudogap in the density of states and by a positive slope in  $\text{Re}\Sigma(\mathbf{k}_F, \varepsilon)$  and a local maximum in  $|\text{Im}\Sigma(\mathbf{k}_F, \varepsilon)|$  at  $\varepsilon = 0$ . We explain these results using a simple spin-fluctuation model.

PACS numbers: 71.27.+a, 75.10.Lp, 75.30.Kz

The 2D single-band Hubbard model plays a central role in efforts to understand the behavior of electrons near the Fermi surface in the cuprate superconductors and their parent compounds [1]. The model is characterized by a nearest-neighbor hopping energy,  $t$ , and an on-site Coulomb energy,  $U$ . For a half-filled band, the  $T = 0$  state is believed to be an antiferromagnetic (AFM) insulator for all  $U > 0$  [2,3]. For  $T > 0$ , the Mermin-Wagner theorem precludes the existence of long-range AFM order in 2D, but with strong coupling ( $U \gtrsim 8t$ ) the low-temperature electronic state is almost certainly a Mott insulator. With  $U = 4t$  and  $0.10t \lesssim T \lesssim 0.25t$ , conflicting results have been obtained from quantum Monte Carlo (QMC) calculations of the one-electron spectral weight function,  $A(\mathbf{k}, \varepsilon)$ , depending on lattice size and especially on the method used to extract  $A(\mathbf{k}, \varepsilon)$  from the Green's function  $G(\mathbf{k}, \tau)$  produced directly by QMC calculations. Spectral functions on the Fermi surface (FS) produced by the maximum entropy technique show a single peak whenever the lattice is larger than the AFM correlation length, but develop a pseudogap on smaller lattices [4]. In contrast, recent calculations using the method of singular value decomposition yield a pseudogap in both the spectral function on the FS and in the total density of states,  $N(\varepsilon) = N^{-1} \sum_{\mathbf{k}} A(\mathbf{k}, \varepsilon)$ , even for lattices larger than the correlation length [5].

We report calculations of  $A(\mathbf{k}, \varepsilon)$  and  $N(\varepsilon)$  at half filling and moderate  $U$  ( $< 4.8t$ ) using the fluctuation exchange approximation (FEA), a self-consistent conserving approximation that has been applied to the 2D Hubbard model in a number of recent papers [6–8]. In particular, the FEA has been used to argue for a  $d$ -wave superconducting transition in the high- $T_c$  cuprates [8]; the need to evaluate these claims adds to the importance of knowing what the FEA predicts (rightly or wrongly) for the normal state at half filling. Compared to QMC, the FEA has the disadvantage that it is inherently an approximation, though imaginary-time Green's functions from the FEA and QMC agree surprisingly well at half filling and moderate  $U$  [6].

For studying the spectral function and density of states (DOS), the FEA has several important advantages over QMC: (1) There is no inherently statistical error in the FEA results, which removes most of the uncertainty in extracting  $A(\mathbf{k}, \varepsilon)$  from  $G(\mathbf{k}, \tau)$ . (2) FEA calculations are possible for large enough lattices (typically  $128 \times 128$ ) to ensure that the profile of  $A(\mathbf{k}, \varepsilon)$  represents the infinite lattice limit, and does not in part reflect the small number of decay channels available to a low-energy quasiparticle on a small lattice. (3) The FEA can cover a wider range of temperatures than are currently accessible to QMC. (4) The FEA provides real-frequency self-energies and fluctuation propagators that explain the origin of structures in  $A(\mathbf{k}, \varepsilon)$  and directly test the applicability of the Fermi liquid picture.

We find that in the FEA a paramagnetic non-Fermi-liquid state evolves with decreasing temperature. The spectral functions on the FS show no pseudogaps over the range of temperatures covered by QMC calculations, but are exceptionally broad. For momenta close to the FS, spectral weight is shifted away from  $\varepsilon = 0$ , producing a weak secondary maximum, which might suggest a “shadow band” [1], although the real part of the denominator of the Green's function still has only a single zero. These features produce a weak pseudogap in the total DOS, even though the FS spectral functions are single peaked [9]. For momenta on or near the FS, the real part of the self-energy has an anomalous positive slope near  $\varepsilon = 0$  and the quasiparticle lifetime has a local minimum there. A simple analytic model shows that these anomalies result from the coupling of quasiparticles to AFM spin fluctuations, without a phase transition to AFM order. The process is anisotropic, beginning at the  $X$  point and spreading over the FS.

The FEA for the self-energy in a paramagnetic state of the Hubbard model is [10]

$$\begin{aligned} \Sigma(\mathbf{r}, \tau) = & U^2 [\chi_{ph}(\mathbf{r}, \tau) + T_{\rho\rho}(\mathbf{r}, \tau) + T_{\sigma\sigma}(\mathbf{r}, \tau)] G(\mathbf{r}, \tau) \\ & + U^2 T_{pp}(\mathbf{r}, \tau) G(-\mathbf{r}, -\tau), \end{aligned} \quad (1)$$

where  $\chi_{ph}(\mathbf{r}, \tau) = -G(\mathbf{r}, \tau)G(-\mathbf{r}, -\tau)$  and  $T_{\sigma\sigma}$ ,  $T_{\rho\rho}$ , and  $T_{pp}$  are propagators for spin fluctuations, density fluctuations, and singlet pair fluctuations. For example, the spin-fluctuation propagator is

$$T_{\sigma\sigma}(\mathbf{q}, \omega_m) = \frac{3}{2} \frac{U\chi_{ph}(\mathbf{q}, \omega_m)^2}{1 - U\chi_{ph}(\mathbf{q}, \omega_m)}. \quad (2)$$

The Green's function is obtained from Dyson's equation,

$$G(\mathbf{k}, \varepsilon_n)^{-1} = G_0(\mathbf{k}, \varepsilon_n)^{-1} - \Sigma(\mathbf{k}, \varepsilon_n), \quad (3)$$

where  $G_0(\mathbf{k}, \varepsilon_n)$  is the noninteracting Green's function, and the self-consistent  $\Sigma$  is found by iteration. We have performed calculations on  $128 \times 128$  lattices of  $\mathbf{k}$  points [11] with typically 512 Matsubara frequencies using a new massively parallel algorithm that treats high frequency contributions exactly [12]. This greatly improved treatment of high-frequency information allows us to obtain what we believe are the first meaningful results for the FEA spectral functions of the Hubbard model at half filling. Numerical analytic continuation of  $\Sigma$  to the real-frequency axis is accomplished using Padé approximants [13].

The extinction of sharp quasiparticles at the  $X$  point is evident from the spectral functions in Fig. 1. For  $U = 1.0$  and  $T = 0.1$ , the FEA solution shows a sharp quasiparticle at  $\varepsilon = 0$ , the Fermi energy (henceforth all energies are in units of  $t$ ). While an increase in the interaction strength and thus an increase in the quasiparticle-quasiparticle scattering rate leads generally to a reduction in spectral weight at  $\varepsilon = 0$  and a broadening of the spectral function, the effect shown for  $U = 2.3$  in Fig. 1 is much larger than expected.

To see this, focus on the self-energies at the  $X$  point shown in Fig. 2. Scaling of the  $U = 1$  result by  $U^2$  leads to an  $\text{Im}\Sigma$  comparable to the  $U = 2.3$  result at high frequency, but smaller than the true self-energy for  $\varepsilon \approx 0$  by a factor of  $\approx 2.5$ . The FEA self-energy at low energy

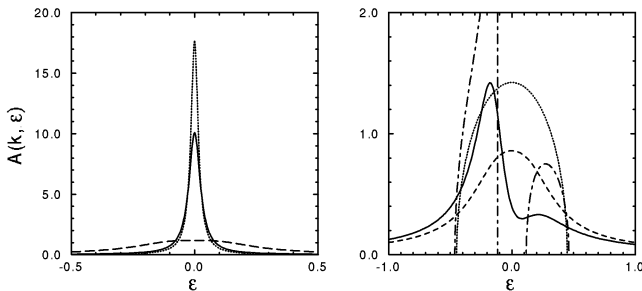


FIG. 1. Left: Spectral functions calculated in the FEA at  $T = 0.10$ , showing a dramatic reduction of spectral weight at the  $X$  point (on the Fermi surface) with a modest increase in  $U$  between  $T = 0.10$  and  $U = 1.0$  (dotted) and  $2.3$  (dashed). Also shown for  $U = 2.3$  (solid) is a calculation with only the second order skeleton diagram. Right: FEA spectral functions for  $\mathbf{k} = (0.891\pi, 0)$  (solid) and  $\mathbf{k} = (\pi, 0)$  (dashed) shown in comparison with those for the simple spin fluctuation model (long-dash-short-dashed and dotted, respectively) for  $\tilde{t}_{sp} = 0.05$ .

is inconsistent with Fermi liquid theory: an anomalous maximum is clearly evident at  $\varepsilon = 0$  in  $|\text{Im}\Sigma|$ , and  $\text{Re}\Sigma$  at  $\varepsilon = 0$  has a positive slope which is inconsistent with the interpretation of  $[1 - \partial \text{Re}\Sigma(\mathbf{k}_F, \varepsilon)/\partial \varepsilon|_{\varepsilon=0}]^{-1}$  as the quasiparticle pole weight. For the same  $U$  a self-consistent calculation with only the second-order skeleton diagram yields a sharp spectral function and self-energies without these anomalies.

The dramatic loss of spectral weight at the Fermi surface is reflected in the formation of a weak pseudogap in the total density of states as a function of temperature as shown for  $U = 1.57$  in Fig. 3. The anomalies in  $\Sigma$  first appear at the Van Hove critical points, and spread as  $T$  decreases; for a range of  $U$  and  $T$ , the anomalous excitations near the  $X$  points coexist with more conventional quasiparticles on the rest of the Fermi surface.

The redistribution of spectral weight away from the Fermi energy is a consequence of strong antiferromagnetic spin correlations, signaled by the growth of sharp structure in the spin-fluctuation  $T$  matrix  $T_{\sigma\sigma}$  when  $U\chi_{ph}(\mathbf{Q}, 0)$  approaches unity at  $\mathbf{Q} = (\pi, \pi)$ . In a Hartree-Fock theory,  $U\chi_{ph}(\mathbf{Q}, 0)$  reaches unity at a sufficiently low temperature, signaling a transition to AFM order. Within the FEA, the self-consistently determined quasiparticle lifetime regulates the growth of  $U\chi_{ph}(\mathbf{Q}, 0)$ . As shown in Fig. 4,  $U\chi_{ph}(\mathbf{Q}, 0)$  closely approaches unity with decreasing temperature at fixed  $U$ , and with increasing  $U$  for fixed  $T$ . As the temperature is decreased for fixed  $U$  a sharply peaked structure evolves in  $T_{\sigma\sigma}(\mathbf{q}, \omega_m)$  within  $|\Delta q| \approx 0.05\pi$  of  $\mathbf{Q}$  (for  $U = 2.7$  and  $T = 0.10$ ) and, to an excellent approximation, at  $\omega_m = 0$ . For real frequencies,  $T_{\sigma\sigma}(\mathbf{Q}, \omega)$  has a sharply peaked structure as shown in Fig. 4. At higher temperatures, as shown for  $T = 0.15$ , temperature and correlations broaden the peak in  $U\chi_{ph}(\mathbf{Q}, 0)$  and

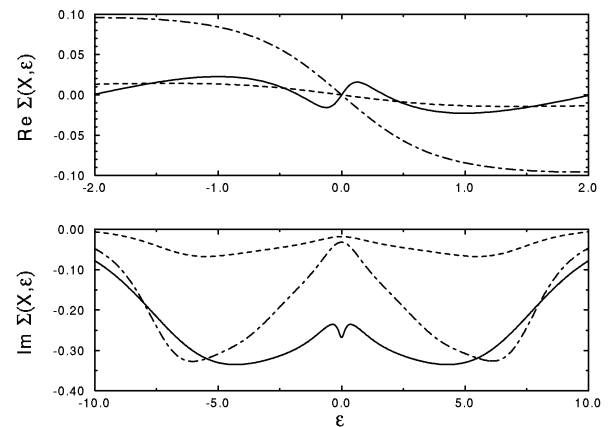


FIG. 2. The real and imaginary parts of the FEA self-energy at the  $X$  point for  $U = 1.0$  (dashed) and  $U = 2.3$  (solid). Note the “inverted peak” at  $\varepsilon = 0$  in the imaginary part and the positive slope at low energy in the real part. Also shown is the self-energy from a self-consistent calculation with only the second-order skeleton diagram for  $U = 2.3$  (dash-dotted) which is qualitatively similar to the FEA for  $U = 1.0$ .

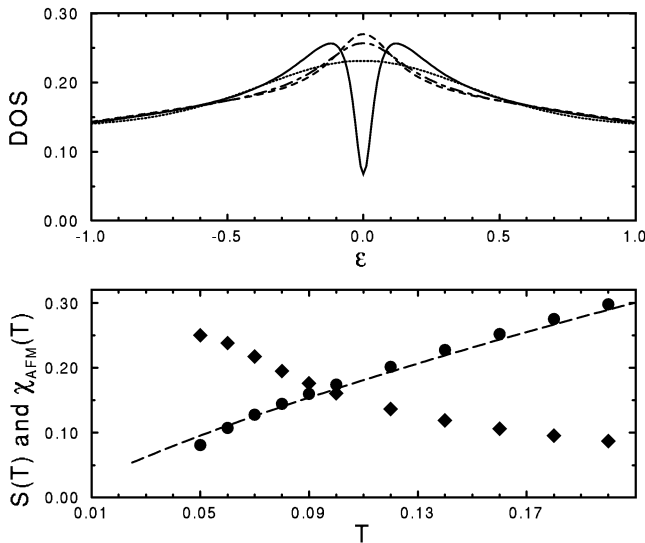


FIG. 3. Top: The density of states as a function of energy for  $U = 1.57$  and  $T = 0.16$  (dashed),  $0.14$  (dash-dotted),  $0.07$  (dotted), and  $0.05$  (solid) showing the evolution of a weak pseudogap with decreasing temperature. Bottom: The self-consistent AFM spin susceptibility (diamonds) and entropy (●) as a function of temperature for  $U = 1.57$ . Also shown is the entropy for  $U = 0$  (dashed). Note that for clarity,  $\chi_{\text{AFM}}(T)$  has been plotted as  $\chi_{\text{AFM}}(T)/4\chi_{\text{AFM}}(0.05)$ . There is no sign of a spin density wave with  $\mathbf{q} = (\pi, \pi)$  in the full spin susceptibility.

hence in  $\text{Re}T_{\sigma\sigma}$  (see Fig. 4, inset) sufficiently that a region of positive slope in  $\text{Re}\Sigma(\mathbf{k}_F, \varepsilon)$  at  $\varepsilon = 0$  is not observed for any  $U$  and only a weak maximum at  $U \approx 4.8$  is evident in  $U\chi_{ph}(\mathbf{Q}, 0)$  as a function of  $U$ .

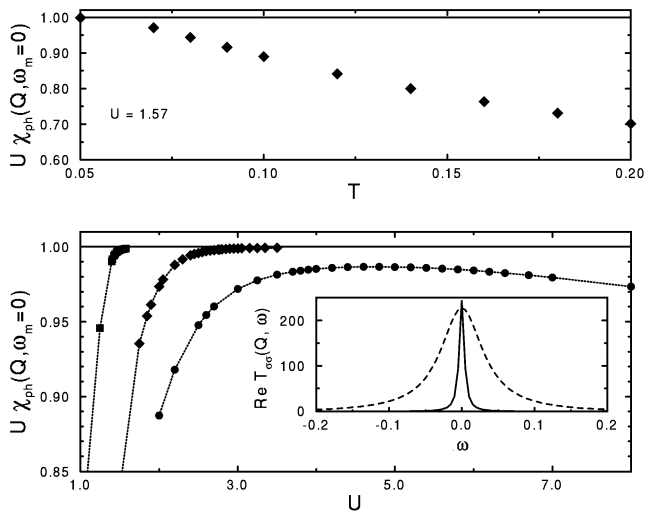


FIG. 4. The self-consistent  $U\chi(\mathbf{Q}, 0)$  (top) for  $U = 1.57$  as a function of  $T$  and (bottom) for  $T = 0.05$  (squares),  $0.10$  (diamonds), and  $0.15$  (●) as a function of  $U$ . The inset shows analytic continuations of the self-consistent  $T$ -matrix  $\text{Re}T_{\sigma\sigma}(\mathbf{Q}, \omega)$  for  $T = 0.10$  and  $U = 2.7$  (solid) and for  $T = 0.15$  and  $U = 4.8$  ( $\times 10$  and dashed). The former shows a pseudogap in the density of states but the latter does not.

At  $T = 0.1$ , further increases in  $U$  lead to neither a positive slope in  $\text{Re}\Sigma$  nor sharp structure in  $\text{Im}\Sigma$  at  $\varepsilon \approx 0$ , perhaps because the large quasiparticle width “smears” the Fermi surface and reduces the effect of nesting and Van Hove critical points. However,  $U\chi_{ph}(\mathbf{Q}, 0)$  continues to approach unity monotonically up to the largest  $U$  ( $\approx 3.6$ ) for which we have solutions at  $T = 0.1$ . Hence it is the sharpness of  $U\chi_{ph}(\mathbf{Q}, 0)$  (and  $T_{\sigma\sigma}$ ) and not simply its size that leads to the observed anomalies.

The entropy  $S$  and AFM susceptibility  $\chi_{\text{AFM}}$  [14] as a function of temperature are shown in Fig. 3 for  $U = 1.57$ . At high temperatures,  $S(T)$  tracks the  $U = 0$  entropy. As the pseudogap opens the entropy turns down, signaling the loss of quasiparticle states. For  $T \approx 0.05$ ,  $\chi_{\text{AFM}}$  shows only a modest enhancement and the paramagnetic state remains stable, as required in 2D. The nearly singular behavior of  $T_{\sigma\sigma}(\mathbf{Q}, 0)$  is offset by the vertex corrections included in a fully conserving description, as suggested by previous calculations [15].

To understand better the self-consistent self-energy, we appeal to a simple model motivated by a calculation of the fluctuation conductivity above  $T_c$  in superconductors [16]. The anomalies in  $\Sigma$  are always accompanied by a  $T_{\sigma\sigma}(\mathbf{q}, \omega_m)$  that is strongly peaked near  $\mathbf{q} = \mathbf{Q}$  and  $\omega_m = 0$  [17]. Assuming that the spin-fluctuation contribution to  $\Sigma$  dominates,

$$\Sigma(\mathbf{k}, \varepsilon_n) \approx G(\mathbf{k} + \mathbf{Q}, \varepsilon_n)\tilde{t}_{sp}, \quad (4)$$

where  $\tilde{t}_{sp}$  is proportional to the weight of the peak in  $T_{\sigma\sigma}$  within a reciprocal correlation length  $\xi^{-1}$  of  $\mathbf{Q}$ ,

$$\tilde{t}_{sp} = \frac{U^2 T}{N} \sum_{|\mathbf{q}| < 1/\xi} T_{\sigma\sigma}(\mathbf{Q} + \mathbf{q}, \omega_m = 0). \quad (5)$$

Equations (4) and (5), together with Dyson’s equation, can be solved directly. For  $\varepsilon \approx 0$  the slope of  $\text{Re}\Sigma(\varepsilon)$  is  $1/2$ . In the full calculation, the slope is also positive when  $T_{\sigma\sigma}$  is sharply peaked, but generally differs from  $1/2$  due to other contributions to the self-energy not included in Eq. (4). We observe that for slopes greater than unity, multiple quasiparticle peaks can appear in the spectral function, corresponding to multiple solutions of  $\varepsilon - \varepsilon_{\mathbf{k}} - \text{Re}\Sigma(\mathbf{k}, \varepsilon) = 0$  for a given wave vector. For  $T \geq 0.05$  we have not observed such a splitting of the band, in contrast to at least two non-self-consistent calculations describing the effects of strong antiferromagnetic correlations on quasiparticle properties [18,19].

The single-particle spectral function for the model is nonzero only for  $0 < \varepsilon_- - \varepsilon_+ < 4\tilde{t}_{sp}$ , and given by

$$A(\mathbf{k}, \varepsilon) = \frac{1}{\pi\tilde{t}_{sp}} \sqrt{\frac{\varepsilon_+}{\varepsilon_-}} \sqrt{\tilde{t}_{sp} - \varepsilon_- - \varepsilon_+/4}, \quad (6)$$

where  $\varepsilon_- = \varepsilon - \varepsilon_{\mathbf{k}}$  and  $\varepsilon_+ = \varepsilon - \varepsilon_{\mathbf{k}+\mathbf{Q}} = \varepsilon + \varepsilon_{\mathbf{k}}$ . This spectral function shares two important features with the full calculation. First, spectral weight at  $\varepsilon_{\mathbf{k}}$  is shifted away from  $\varepsilon = 0$ , with the noninteracting delta function peak becoming a square root singularity truncated at  $\varepsilon_{\mathbf{k}}$ .

This transfer of spectral weight from  $\varepsilon = 0$  leads to the formation of a pseudogap in the total density of states similar to the FEA pseudogap shown in Fig. 3. Second, an additional peak forms at  $\varepsilon_{\mathbf{k}+\mathbf{Q}}$  as expected from dynamical coupling to antiferromagnetic spin fluctuations. We emphasize that  $\varepsilon_{\mathbf{k}+\mathbf{Q}} - \varepsilon_{\mathbf{k}} - \text{Re}\Sigma(\mathbf{k}, \varepsilon_{\mathbf{k}+\mathbf{Q}}) \neq 0$  so that this second peak is not a second quasiparticle solution. Spectral functions for  $\tilde{t}_{sp} = 0.05$ , a value consistent with  $T_{\sigma\sigma}(\mathbf{q}, \omega_m)$  for  $U = 2.7$  and  $T = 0.10$ , are shown together with those from the full FEA calculation in Fig. 1. Given the simplicity of the approximation, the agreement is good. Results obtained from analytic continuation of quantum Monte Carlo data at low temperature ( $T = 0.1$ ) and moderate coupling ( $U = 4$ ) appear consistent with these general features [20].

In summary, the FEA yields thermally broadened quasiparticles at high  $T$  for any  $U \leq 8t$ . With decreasing temperature and for a modest  $U$ , a sharply peaked spin fluctuation propagator develops, whose coupling to the evolving quasiparticle excitations leads to a radical breakdown of Fermi liquid theory and to a weak pseudogap in the single-particle DOS, in the absence of AFM order or of a gap in the spectral functions on the Fermi surface.

This work was supported in part by a grant of computer time from the Office of Naval Research and the DOD HPC Shared Resource Centers: Naval Research Laboratory Connection Machine Facility CM-5; Army High Performance Computing Research Center, under the auspices of Army Research Office Contract No. DAAL03-89-C-0038 with the University of Minnesota.

- 
- [1] For a review of recent numerical work, see E. Dagotto, *Rev. Mod. Phys.* **66**, 763 (1994).  
 [2] J. E. Hirsch and S. Tang, *Phys. Rev. Lett.* **62**, 591 (1989).  
 [3] S. R. White, D. J. Scalapino, R. L. Sugar, E. Y. Loh, S. E. Gubernatis, and R. T. Scalettar, *Phys. Rev. B* **40**, 506 (1989).

- [4] S. R. White, *Phys. Rev. B* **44**, 4670 (1991); M. Vekić and S. R. White, *ibid.* **47**, 1160 (1993).  
 [5] C. E. Creffield, E. G. Klepfish, E. R. Pike, and Sarben Sarkar, *Phys. Rev. Lett.* **75**, 517 (1995).  
 [6] N. E. Bickers, D. J. Scalapino, and S. R. White, *Phys. Rev. Lett.* **62**, 961 (1989).  
 [7] T. Dahm and L. Tewordt, *Phys. Rev. Lett.* **74**, 793 (1995).  
 [8] Chien-Hua Pao and N. E. Bickers, *Phys. Rev. Lett.* **72**, 1870 (1994); P. Montheux and D. J. Scalapino, *ibid.* **72**, 1874 (1994).  
 [9] It is interesting to note that at  $T = 0.05$  a slight depression in  $A(\mathbf{k}, \varepsilon)$  at  $\varepsilon = 0$  is apparent, suggesting incipient pseudogap formation.  
 [10] See, e.g., J. W. Serene and D. W. Hess, in *Recent Progress in Many-Body Theories*, edited by T. L. Ainsworth *et al.* (Plenum, New York, 1992), Vol. 3.  
 [11] A fine mesh is required to represent accurately sharp structure in the spin-fluctuation propagator with decreasing temperature.  
 [12] J. J. Deisz, D. W. Hess, and J. W. Serene, in "Recent Progress in Many-Body Theories," edited by E. Schachinger *et al.* (Plenum, New York, to be published), Vol. 4.  
 [13] H. J. Vidberg and J. W. Serene, *J. Low Temp. Phys.* **19**, 179 (1977).  
 [14] The self-consistent AFM response was found with the method of P. G. McQueen *et al.*, *Phys. Rev. Lett.* **71**, 129 (1993).  
 [15] N. E. Bickers and S. R. White, *Phys. Rev. B* **43**, 8044 (1991).  
 [16] B. R. Patton, Ph.D. thesis, Cornell University, 1971 (unpublished); B. R. Patton, *Phys. Rev. Lett.* **27**, 1273 (1971).  
 [17] Isolating the  $\omega_m = 0$  term distinguishes this regime from the frequency-independent spin-density-wave approximation [J. R. Schrieffer, X.-G. Wen, and S.-C. Zhang, *Phys. Rev. B* **39**, 11 663 (1989)].  
 [18] A. P. Kampf and J. R. Schrieffer, *Phys. Rev. B* **42**, 7967 (1990).  
 [19] P. de Vries, K. Michielsen, and H. De Raedt, *Z. Phys. B* **95**, 475 (1994).  
 [20] S. R. White, *Phys. Rev. B* **44**, 4670 (1991).